engineering proceedings

MDPI

Proceeding Paper

The Effect of Twisted Baffle on the Microbubble Generator Swirl Ventury Type †

Fatma Roshanti [1], Sigit Deddy Purnomo Sidhi [1,2], Samsul Kamal [1,3], Deendarlianto [1,3,*] and Indarto [1,3]

[1] Department of Mechanical and Industrial Engineering, Universitas Gadjah Mada; email1@email.com (F.R.); email2@email.com (S.D.P.S.); email3@email.com (S.K.); email4@email.com (I.)
[2] Fishing Mechanization, Politeknik Perikanan dan Kelautan Sorong
[3] Center of Energy Studies, Universitas Gadjah Mada
* Correspondence: deendarlianto@ugm.ac.id
† Presented at the 2nd International Electronic Conference on Processes: Process Engineering—Current State and Future Trends (ECP 2023), 17–31 May 2023; Available online: https://ecp2023.sciforum.net/.

Abstract: Due to their unique physical properties, microbubbles have received a lot of attention in waste treatment, aquaculture, and food processing. The demand for high-efficient and low-power consumption microbubble generators has become a challenge today. Swirling flow has been widely proven that it can improve bubble formation. Numerous researchers have developed designs to produce swirl flow and strengthen the turbulence fluid flow. In this study, we present a swirl venturi microbubble generator with a 60° twisted baffle fin on the inlet section. The performance of the microbubble generator swirl venturi type was tested experimentally using parameters such as distribution of bubble size, hydraulic power (L_w), and bubble-generating efficiency (η_b). A microbubble generator was installed in the transparent test pool with 672 L of water. A high-speed video camera was employed to visualize the flow behaviour. The water and gas flow rates varied between 40–60 lpm and 0.1–0.5 lpm, respectively. The data were analyzed by MATLAB R2022b with the technique image processing method. The results show that most bubbles with 100–300 μm were generated. An increased water flow rate (Q_L) will increase the hydraulic power by 22–27 W, while an enlargement of gas flow rate (Q_G) will only enlarge 1 W. As the water flow rate increases, bubble-generating efficiency decreases. The lowest bubble-generating efficiency of 0.04% occurs at a Q_L 60 lpm and Q_G of 0.1 lpm. In conclusion, we can conclude that the microbubble generator swirl ventury type is an efficient device for generating microbubbles.

Keywords: ventury microbubble generator; swirl; pressure drop; hydraulic power; bubble generating efficiency

Citation: Roshanti, F.; Sidhi, S.D.P.; Kamal, S.; Deendarlianto; Indarto The Effect of Twisted Baffle on the Microbubble Generator Swirl Ventury Type. *Eng. Proc.* **2023**, *37*, x. https://doi.org/10.3390/xxxxx
Published: 17 May 2023

1. Introduction

Microbubble has been enormous applied due to their reliable physical properties. A larger gas-liquid interfacial area, slow-moving in the water, and high self-pressurizing effect are unique microbubble characteristics. The advantages of microbubbles are suitable to enhance dissolved oxygen in the water. It can be used to purify water, aquaculture, and agriculture [1]. The technology that can generate microbubbles is called a microbubble generator. Ventury is one type of microbubble generator. Venturi has no complicated structure, low energy consumption, and no internal rotating parts [2]. Bubbles will form due to self-suction due to vacuum pressure in the throat and reduction in cross-sectional area. The bubbles formed will then be deformed into small shapes.

The fluid flow rate affects the performance of the microbubble generator [3,4]. Several modifications, such as the addition of spiral fins [5], porous media [6], combined with orifices [7], have been made to increase the efficiency of the ventury. Several modifications on the divergent and convergent sides of the microbubble generator have been conducted

by the researchers, but modifications at the inlet are still not widely carried out. For this reason, this research will evaluate the performance of the microbubble generator on bubble diameter, pressure drop, hydraulic power, and bubble-generating efficiency.

2. Materials and Methods

Figure 1 depicts the experimental apparatus used in this study. Four twisted fin baffles with a 60° angle twisted on the inlet section ventury were employed in this study, as shown in Figure 2. It has a 29 mm inlet diameter and is placed 0.2 m from the bottom of an aquarium. A total of 15 tests were run by varying water flow rate (Q_L) from 40–60 lpm and gas flow rate (Q_G) from 0.1–0.5 lpm.

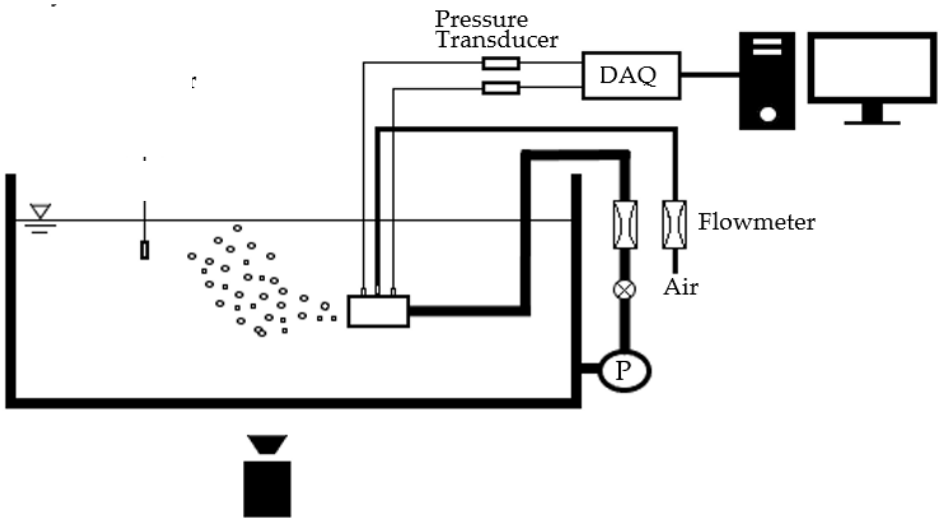

Figure 1. Sistem experimental apparatus.

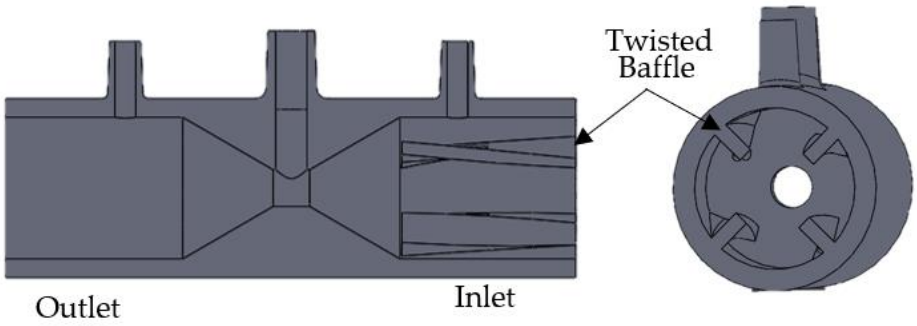

Figure 2. Swirl Venturi Microbubble Generator.

This study used a high-speed video camera (Phantom Miro M310) to visualize bubble behaviour under several testing conditions. The camera was set at a resolution of 768 × 480 with a recording speed of 3000 fps. The experimental data was obtained using an image processing technique adapted by previous research [7]. A differential pressure transducer Validyne P55D was installed at the ventury inlets and outlets section to evaluate pressure drop. To collect pressure data, Advantech data acquisition is used. Pressure drop, hydraulic power, and bubble-generating efficiency parameters can be calculated using this equation [8]:

$$\Delta P = P_2 - P_1 \quad (1)$$

$$L_w = (P_1 + \varrho_L \cdot v_{L1}^2)Q_L \quad (2)$$

$$\eta_B = (\varrho_L \cdot g \cdot H \cdot Q_G)L_w \quad (3)$$

where subscripts 1 and 2 mean inlets and outlets. ϱ_L is the water density, v_{L1} represents the water velocity before entering the reduction area, and H is the position microbubble generator from the water surface.

3. Results and Discussion

This chapter will discuss the analysis by parameter bubble size distribution, pressure drop, hydraulic power (L_w), and bubble-generating efficiency (η_B) from obtained experimental data. Bubble size distribution was analyzed with an image processing toolbox in MATLAB R2022b. Meanwhile, hydraulic power and bubble-generating efficiency were analyzed from differential pressure data. Variation water and gas flow rates were conducted in this study.

3.1. Distribution of Bubble Size

The size of the bubble is an important indicator in a microbubble generator. This section thoroughly compared the effects of liquid-gas flow rates on bubble size distribution. Figure 3 provides the distribution of bubble sizes in distinct flow scenarios. The visualization shows that the water flow rate of 60 lpm produces smaller and more uniform bubbles than the water flow rate of 40 and 50 lpm.

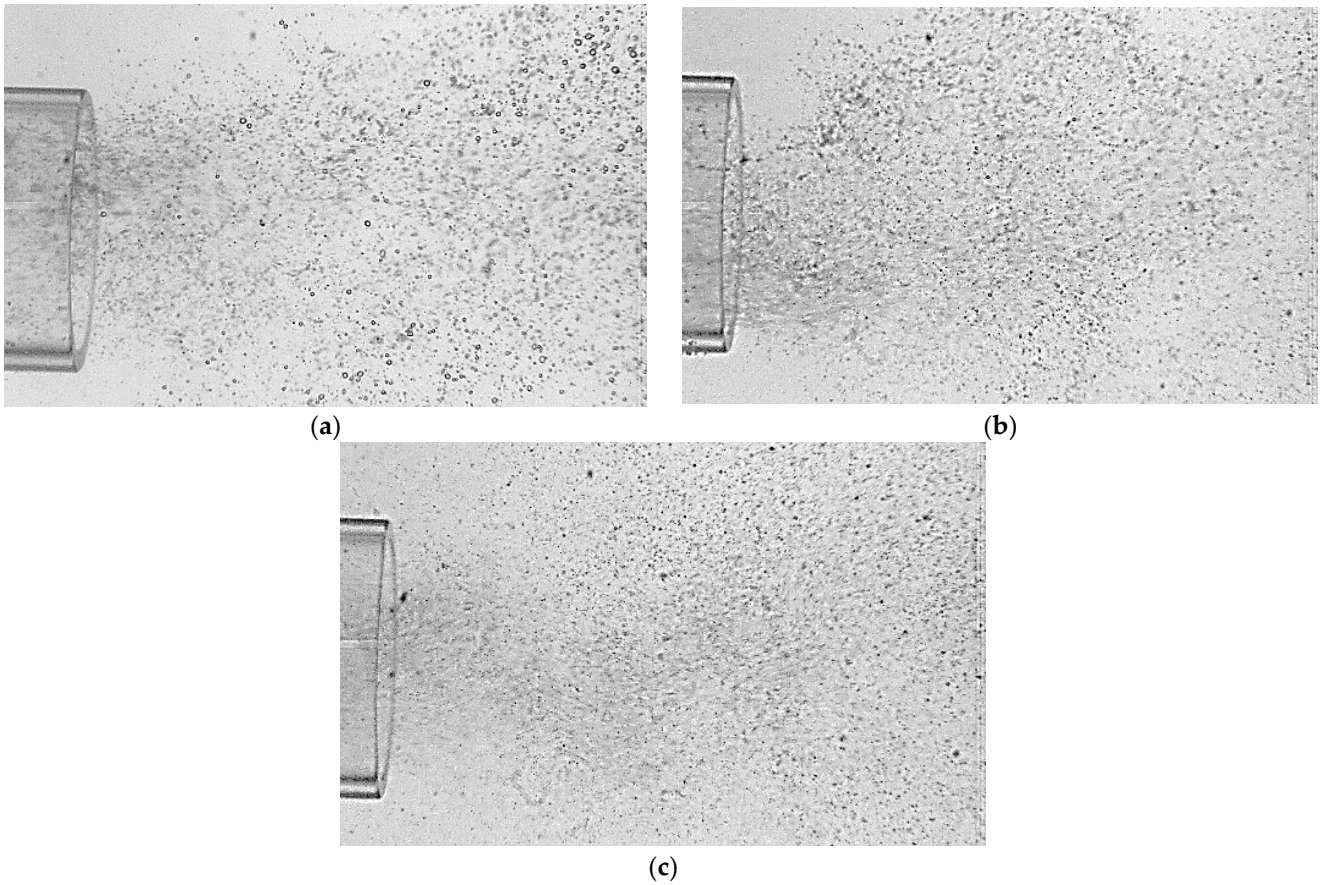

Figure 3. Bubble distribution at (**a**) Q_L = 40 lpm; (**b**) Q_L = 50 lpm; (**c**) Q_L = 60 lpm.

The distribution of bubble size will express in the probability density function (PDF). From Figure 4, it was found that the bubble had generated in 100–300 μm diameter. A higher probability graphic reached 0.385 at Q_L 60 lpm. An increase in water flow rate increases water velocity and inertia forces. When inertia surpasses Weber's force, a larger

shear stress is applied to the bubble and breaks it into pieces. In addition, enlarging the water flow rate will inhibit initial bubble formation so that the average bubble diameter will decrease.

In the meantime, enlargement of the gas flow rate should diminish bubble stability while increasing the effect of bubble coalescence. Coalescence is defined as forming large bubbles from small ones [9]. Colaessence decreases probability curve distribution. This statement is in line with previous work [4,6].

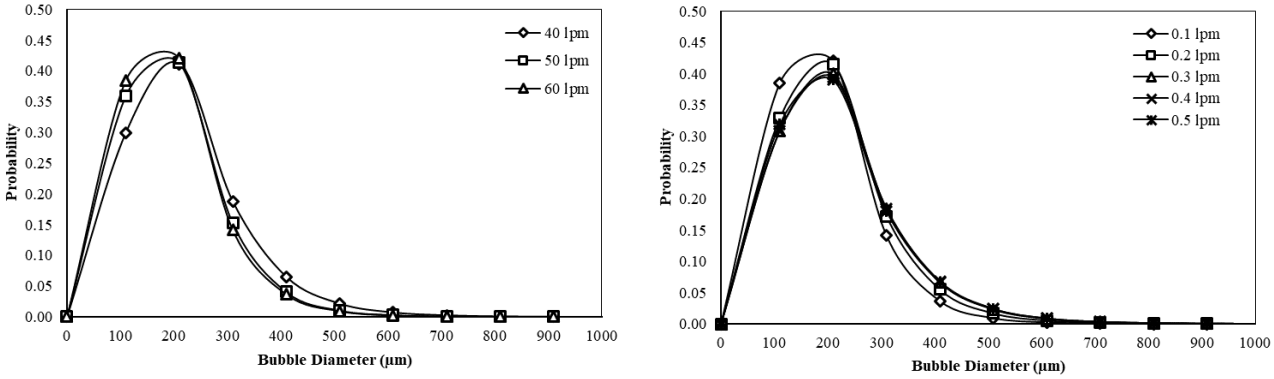

Figure 4. Bubble size distribution at (**a**) Q_G = 0.1 lpm; (**b**) Q_L = 60 lpm.

3.2. Pressure Drop (ΔP)

Data pressure from physical experiments will be calculated by Equation (1). A combination of Q_L and Q_G has a distinct response. Figure 5 demonstrates that pressure drops are linearly increased with increasing water flow rates. The tiniest pressure drop occurred at a 40 lpm water flow rate. In contrast, the enhancement of gas flow rate is not significantly affected pressure drop. It can be seen where the curves during the variation of gas flow rates created an identical graphic.

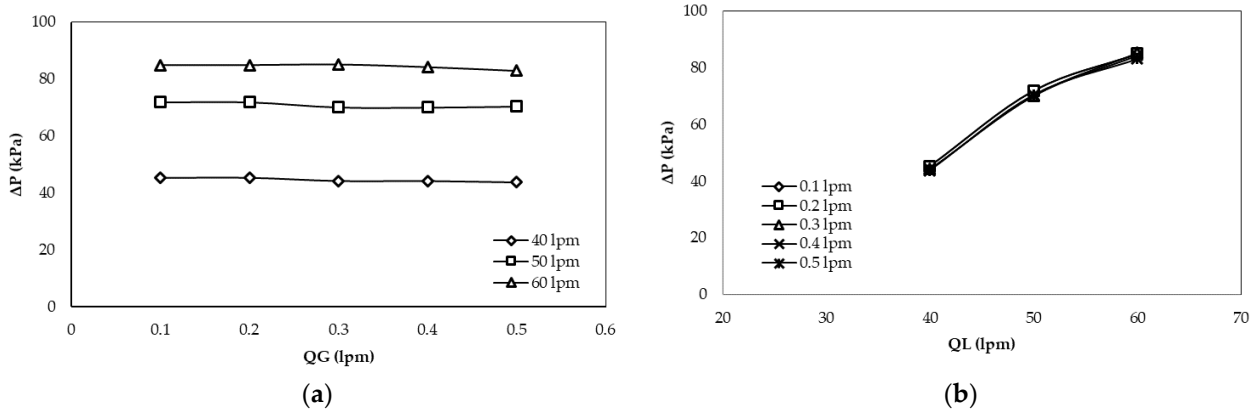

Figure 5. Pressure drop at (**a**) Q_G constant; (**b**) Q_L constant.

3.3. Hydraulic Power (L_w)

Figure 6 compares the calculated hydraulic power for Q_L and Q_G variations. Higher hydraulic power occurred at Q_L 60 lpm by 79.04 W. L_w increased linearly with pressure drop and water flow rates. An increased water flow rate (Q_L) will increase the hydraulic power by 22–27 W, while an increase in gas flow rate (Q_G) will only increase 1 W and conduce almost the same graphic. So, we can conclude that the water flow rates more significantly affected L_w than gas flow rates.

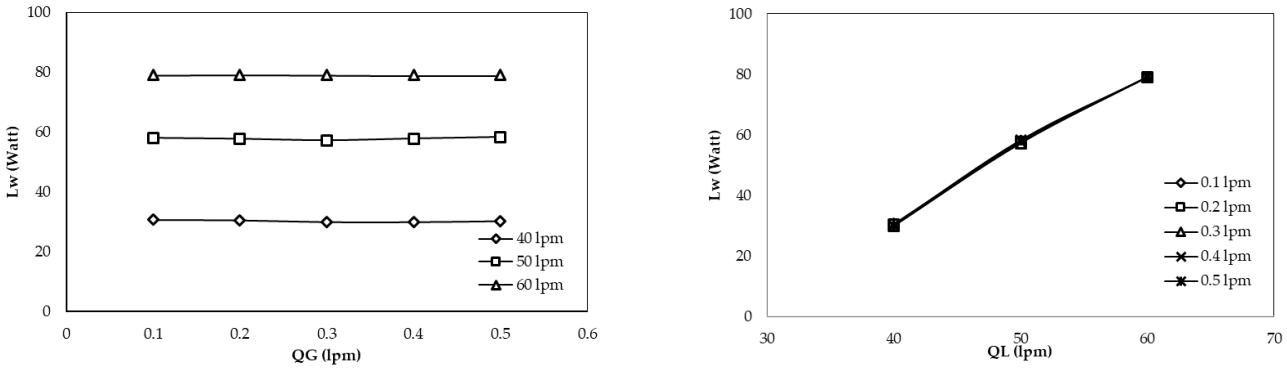

Figure 6. Hydraullic power at (**a**) Q_G constant; (**b**) Q_L constant.

Hydraulic power represents stored energy in the water flow in a microbubble generator. The lower the hydraulic power, the better the performance, and it is easy to select a water circulation pump [8].

3.4. Bubble-Generating Efficiency (η_B)

Bubble-generating efficiency means the energy received by air from water flow rates. Figure 7 displays the relationship between variation Q_G and Q_L by bubble-generating efficiency. It can be seen that the smallest bubble-generating efficiency occurred at Q_L 60 lpm on Q_G 0.1–0.5 lpm. On the other hand, η_B proportionally with the increment of gas flow rates. The highest η_B reached 0.05% at Q_G 0.5 lpm.

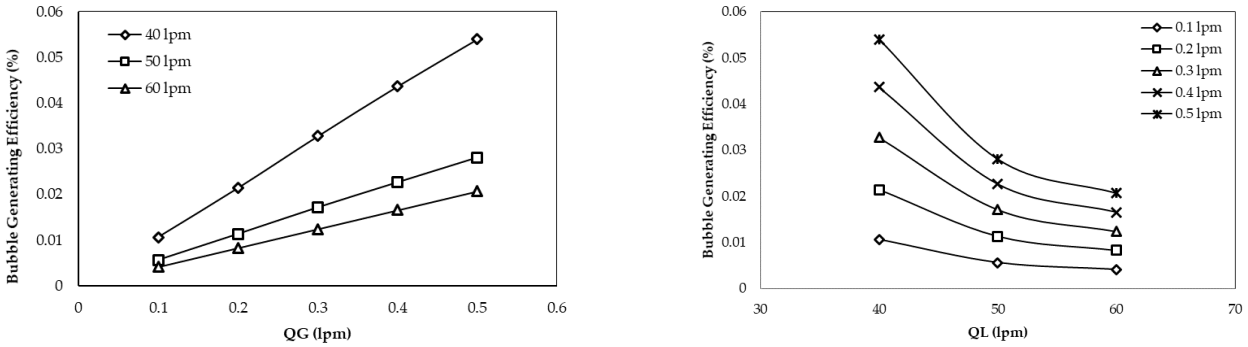

Figure 7. Bubble Generating efficiency at (**a**) Q_G constant; (**b**) Q_L constant.

If compared, the bubble-generating efficiency in this study has lower η_B than the spherical body and porous venturi microbubble generator [6,9]. Bubble-generating efficiency decreases with an increase in hydraulic power. The lower η_B indicates that energy inside the water is used to break air into a tiny bubble in the microbubble generator rather than suck air into it [8].

4. Conclusions

The addition of the twisted baffle on the ventury microbubble generator was analyzed by examining the bubble size distribution, pressure drop (ΔP), hydraulic power (L_w), and bubble-generating efficiency (η_B). As a result, we found that bubbles with a diameter of 100–300 μm were generated. Bubble size diameter increase as Q_G increase, while inversely with Q_L. Hydraulic power increase linearly with pressure drop and Q_L. The higher L_w decrease in η_B improved the performance of the microbubble generator. Further

investigation is required to discover dissolved oxygen concentration, SAE, SOTR, and SOTE.

Author Contributions: F.R. experimental measurements and writing the original draft. S.D.P.S. conceptualization, experimental measurements S.K. writing—review & editing. D. supervision, writing, formal analysis. I. supervision, writing, formal analysis. All authors have read and agreed to the published version of the manuscript.

Data Availability Statement: The information reported in this study will be made available upon request.

Acknowledgments: We acknowledge the Department of Mechanical and Industry Engineering, Universitas Gadjah Mada, for the support throughout the work.

References

1. Tsuge, H. *Micro and Nanobubbles Fundamentals and Applications*; 1st ed.; Taylor & Francis: Boca Raton, FL, USA, 2015.
2. Huang, J.; Sun, L.; Liu, H.; Mo, Z.; Tang, J.; Xie, G.; Du, M. A review on bubble generation and transportation in Venturi-type bubble generators. *Exp. Comput. Multiph. Flow* **2020**, *2*, 123–134. https://doi.org/10.1007/s42757-019-0049-3.
3. Deendarlianto; Wiratni; Tontowi, A.E.; Indarto; Iriawan, A.G.W. The implementation of a developed microbubble generator on the aerobic wastewater treatment. *Int. J. Technol.* **2015**, *6*, 924–930. https://doi.org/10.14716/ijtech.v6i6.1696.
4. Gordiychuk, A.; Svanera, M.; Benini, S.; Poesio, P. Size distribution and Sauter mean diameter of micro bubbles for a Venturi type bubble generator. *Exp. Therm. Fluid Sci.* **2016**, *70*, 51–60. https://doi.org/10.1016/j.expthermflusci.2015.08.014.
5. Shin, D.H.; Gim, Y.; Sohn, D.K.; Ko, H.S. Development of venturi-tube with spiral-shaped fin for water treatment. *J. Fluids Eng. Trans. ASME* **2019**, *141*, 051303. https://doi.org/10.1115/1.4042750.
6. Majid, A.I.; Nugroho, F.M.; Juwana, W.E.; Budhijanto, W.; Deendarlianto; Indarto. On the performance of venturi-porous pipe microbubble generator with inlet angle of 20° and outlet angle of 12°. *AIP Conf. Proc.* **2018**, *2001*, 050009. https://doi.org/10.1063/1.5050000.
7. Juwana, W.E.; Widyatama, A.; Dinaryanto, O.; Budhijanto, W.; Indarto; Deendarlianto. Hydrodynamic characteristics of the microbubble dissolution in liquid using orifice type microbubble generator. *Chem. Eng. Res. Des.* **2019**, *141*, 436–448. https://doi.org/10.1016/j.cherd.2018.11.017.
8. Sadatomi, M.; Kawahara, A.; Kano, K.; Ohtomo, A. Performance of a new micro-bubble generator with a spherical body in a flowing water tube. *Exp. Therm. Fluid Sci.* **2005**, *29*, 615–623. https://doi.org/10.1016/j.expthermflusci.2004.08.006.
9. Levitsky, I.; Tavor, D.; Gitis, V. Micro and nanobubbles in water and wastewater treatment: A state-of-the-art review. *J. Water Process Eng.* **2022**, *47*, 102688. https://doi.org/10.1016/j.jwpe.2022.102688.